NATIONAL ADVISORY COMMITTEE FOR AERONAUTICS

TECHNICAL NOTE 4153

EFFECT OF WALL COOLING ON INLET PARAMETERS OF A SCOOP OPERATING IN A TURBULENT BOUNDARY LAYER ON A FLAT OR CONICAL SURFACE FOR MACH NUMBERS 2 TO 10

By Andrew Beke

Lewis Flight Propulsion Laboratory
Cleveland, Ohio

Washington
March 1958

NATIONAL ADVISORY COMMITTEE FOR AERONAUTICS

TECHNICAL NOTE 4153

EFFECT OF WALL COOLING ON INLET PARAMETERS OF A SCOOP OPERATING IN A TURBULENT BOUNDARY LAYER ON A FLAT OR CONICAL SURFACE FOR MACH NUMBERS 2 TO 10

By Andrew Beke

SUMMARY

Analytical results were obtained for boundary-layer mass flow, momentum, total-temperature, and total-pressure recovery ratios of a scoop inlet with a height equal to the boundary-layer thickness and operating in a turbulent boundary layer, for flat and conical surfaces with wall cooling. When the wall temperature is reduced from the adiabatic temperature to that of the free-stream static temperature, mass-flow and momentum ratios increase up to 50 percent, while the total-temperature ratio of this airflow is reduced by about 6 percent, and the total-pressure recovery increases slightly.

INTRODUCTION

At low supersonic speeds boundary-layer scoop inlets may be considered as operating in the region of no heat transfer or near insulated walls. The performance characteristics for this case have been presented for the flat plate in reference 1. At high supersonic speeds, however, aerodynamic heating becomes significant, and wall cooling may be necessary to maintain the structural and aerodynamic integrity of the aircraft. Theoretical studies of wall cooling related to this problem have been made in references 2 and 3. Since boundary-layer auxiliary inlets may have to operate in flight areas where wall cooling is required, it therefore becomes necessary to acquire knowledge of the effect of wall cooling on the performance characteristics of boundary-layer scoop inlets.

The theoretical analyses for a turbulent-compressible boundary layer with heat transfer from references 2 and 3 (where the Prandtl number is assumed equal to unity) were applied to a method similar to that used in reference 1 in order to determine the mass-flow, momentum, total-pressure, and total-temperature ratios for a scoop inlet having a height equal to

the boundary-layer thickness. Variations of these inlet parameters, for flat and conical surfaces, are presented for several wall-to-free-stream static-temperature ratios and for Mach numbers from 2 to 10.

ANALYSIS

The symbols used in this analysis are presented in appendix A. The method used for obtaining the critical mass-flow and momentum ratios for a boundary-layer scoop inlet with wall cooling is outlined in detail in appendix B. The derivation of these expressions is similar to that for the adiabatic wall (ref. 1), except for the inclusion of the density variation in the boundary layer with various amounts of cooling as indicated by wall surface temperatures. Variation of the boundary-layer temperature and velocity profile as theoretically derived in reference 2 was incorporated in the integration for a scoop inlet having a height equal to the boundary-layer thickness. The Mach number was varied from 2 to 10 for a Reynolds number range from 10^6 to 10^9. For wall-to-free-stream temperature ratios, the temperature of the wall was allowed to vary from the temperature for local free-stream to that for an adiabatic wall. Of course, these adiabatic temperatures are for a recovery factor of unity and perhaps are not representative of the real flow case. Since changing the Prandtl number from 0.75 to unity had little effect on the adiabatic skin friction coefficient (ref. 2), the recovery factor for the real flow case ($r = 0.9$, turbulent flow) was used in order to obtain the variations of mass flow and momentum ratio for this condition.

Since heat is transferred from the boundary layer when the wall temperatures are less than the adiabatic value, the scoop inlet total-temperature ratio and total pressure will be changed. The total-temperature ratio will vary with Mach number, wall temperature, mass flow, and momentum of the boundary-layer air as shown in appendix B (eq. (B20)). Use of this total-temperature ratio in the one-dimensional mass-flow and momentum equation yields the inlet total-pressure recovery for a normal shock-type inlet in a region of wall cooling (eq. (B23), appendix B). Pressure recoveries were computed for the adiabatic wall value and for the wall static temperature equal to the free-stream temperature.

Extension of equations (B15) and (B16) for the mass-flow and momentum ratios were applied to a cone by using the rule of reference 3, which states that the local heat-transfer coefficient on a cone is the flat plate coefficient for a Reynolds number equal to one-half the Reynolds number on the cone when the Mach number and wall-to-free-stream temperature remain the same. Inasmuch as the boundary-layer temperature distributions derived in reference 2 are general for a surface without a pressure gradient, these distributions may be employed for the cone as well as for the flat-plate case, so that integration of the inlet parameters of appendix B was carried out without changing the form of the integrands of appendix B. These calculations for the cone, of course, yield identical results as for the flat plate.

In order to apply the results of the calculations of appendix B to cases involving boundary-layer airflow scoops, it is necessary to ascertain the variation of the boundary-layer thickness with heat transfer. Derivation of the adiabatic-to-cooled boundary-layer thickness ratio is presented in appendix C for both the flat plate and the cone. The flat-plate boundary-layer thickness ratio may be found from the mean skin friction coefficients of reference 2 and the inlet mass-flow and momentum parameters of appendix B (shown in appendix C (eq. (C3)). Evaluation of the boundary-layer thickness for the conical case (eq. (C4)) only requires the use of the mass-flow and momentum ratios of appendix B and the mean skin-friction coefficients for the cone. These skin-friction values may be found from reference 2 with the condition that the conical value of the mean skin-friction coefficient be that of the flat plate taken at one-half the Reynolds number of the cone.

DISCUSSION OF RESULTS

The theoretical curves for mass-flow and momentum ratios for the flat and conical surfaces are presented in figure 1. At given Reynolds and Mach numbers, the boundary-layer inlet mass-flow and momentum ratios increase with decreased wall-to-free-stream static-temperature ratios. For example, in figure 1(a), at a Reynolds number of 10^6, the increases in mass flow due to wall cooling vary from 10 to 50 percent for the Mach number and cooling range considered. In most cases, at a given Mach number, increasing the Reynolds number reduced the effect of wall cooling. Comparison of the adiabatic mass-flow and momentum ratios of figure 1 with the results of reference 1 indicates fair agreement. Also, as seen in the figure, the variation of the mass flow and momentum ratio for the actual gas flow case ($r = 0.9$) does not differ significantly from the case for a Prandtl number of unity (adiabatic wall condition).

Removing heat from the boundary layer, of course, reduces the mean total temperature of the boundary-layer air. Figure 2 indicates that (for both the cone and flat plate) the effect of extreme wall cooling on the inlet total-temperature ratio is small. For a wall-to-free-stream static-temperature ratio of unity the largest temperature change is about 6 percent at a Reynolds number of 10^6. As the Reynolds number is increased, the temperature ratio increases towards unity.

Figure 3 presents estimates of the variation of scoop pressure recovery with Mach and Reynolds numbers and wall cooling. For a given Reynolds number, the total-pressure ratio with or without cooling drops off rapidly with increased Mach number, while some variation in absolute magnitude exists due to cooling. These trends apparently exist for the whole range of Reynolds numbers investigated. A small variation in the pressure-recovery ratio exists at the various Reynolds numbers for Mach numbers up to about 4. However, a significantly large variation above this speed range does not exist.

Due to the high temperatures which may be reached in the boundary layer at the higher Mach number (M = 10) for the adiabatic case, a deviation of the ratio of specific heats (γ) of the gas in the boundary layer from that of ideal air may be expected. Values of γ equal to 1.1, 1.2, and 1.3 were selected, and the deviation from the ideal gas case was attained for the inlet parameters of figures 1 to 3. Results of these computations are presented in table I. As seen in table I, changing the ratio of specific heats from 1.4 to 1.1 increases the mass-flow, momentum, and total-pressure ratios by about 80, 75, and 70 percent, respectively. The total effect of change in R, and viscosity in the expression for density and velocity distributions of reference 1 is not included and is considered outside the scope of the report.

Although the case for $\gamma = 1.1$ has been discussed previously, it is necessary to point out that the actual average ratio of specific heats for the adiabatic case (M = 10) in the boundary layer can be considerably higher than $\gamma = 1.1$, because the mass in the high shear layer (and, consequently, at the highest temperature) near the wall may only be about 20 percent of the total boundary-layer airflow. The larger portion of the airflow will be at a much lower temperature.

In order that a vehicle maintain its aerodynamic and structural characteristics at M = 10, it is realized that the walls of the vehicle must be cooled to lower temperatures (about 2500° R). Thus, in the practical case, deviation of γ from 1.4 is not too large for cooled wall conditions. The computations for those lower wall temperatures in figures 1 to 3 representing the ideal gas case would therefore apply without significant variation from the actual gas conditions.

CONCLUDING REMARKS

Analysis of the effect of boundary-layer heat transfer on scoop inlet performance indicated that for wall-to-free-stream static-temperature ratios of unity, mass flow and momentum are up to 50 percent higher than for an adiabatic flat plate or conical surface. Associated with these changes are a total-temperature decrease up to 6 percent and a small increase in total-pressure recovery.

In view of these significant variations of boundary-layer airflow properties, design of boundary-layer intake devices or diverters must therefore reflect the effects of wall cooling by either variable or compromised size. Furthermore, drag estimates of such systems must take into account the significant variations which result from wall cooling.

Lewis Flight Propulsion Laboratory
National Advisory Committee for Aeronautics
Cleveland, Ohio, September 10, 1957

APPENDIX A

SYMBOLS

A	area, sq ft
$\frac{A_*}{A}$	isentropic area ratio
a	$\sqrt{\left(\frac{B}{2G}\right)^2 + 1}$, appendix B
B	$\left[\frac{\left(1 + \frac{\gamma - 1}{2} M_0^2\right)}{(t_w/t_0)}\right] - 1$, appendix B
b	inlet-scoop height, ft
C_f	mean skin-friction coefficient
$C_{H,0}$	local heat-transfer coefficient, $\frac{h}{c_p \rho_0 u_0}$
c_f	local skin-friction coefficient
c_p	specific heat at constant pressure 0.241 for air, Btu/(lb)($^\circ$R)
F/F_*	impulse ratio, as defined in appendix B
G	$\sqrt{\frac{\gamma - 1}{2} M_0^2 \Big/ \frac{t_w}{t_0}}$, appendix B
H	total heat transferred, Btu/sec
h	film coefficient of heat transfer, $\frac{q_w}{T_0 - t_w}$, $\frac{\text{Btu}}{(\text{sec})(\text{sq ft})(^\circ\text{R})}$
M	Mach number
m	mass-flow rate, slugs/sec
N	$2.50\sqrt{\frac{M_0^2}{5} C_{H,0}}$, appendix B
$\mathcal{N}$	velocity profile parameter (N of ref. 1)
P	total pressure, lb/sq ft

p	static pressure, lb/sq ft
Q	as defined in equation (B16a), appendix B
q	heat transferred locally, Btu/(sq ft)(sec)
r	recovery factor
R	gas constant, ft-lb/lb-^{o}R
Re	Reynolds number, $\frac{\rho_{o}u_{o}x}{\mu_{o}}$
T	total temperature, ^{o}R
t	static temperature, ^{o}R
u	velocity, ft/sec
v	as defined in equation (B10), appendix B
x	longitudinal distance along surface of flat plate or cone, ft
y	distance normal to surface, ft
α	as defined in equation (B11a), appendix B
γ	ratio of specific heats for air, 1.4
δ	boundary-layer (velocity) thickness, ft
θ	cone semivertex angle, deg
μ	coefficient of viscosity for air, (lb)(sec)/(sq ft)
ρ	mass density of air, slugs/cu ft
τ	shear stress, lb/sq ft
Φ	total momentum, $pA(1 + \gamma M^{2})$, lb
φ	momentum, $\rho u^{2}A$, lb

Subscripts:

ad	adiabatic wall conditions
bl	boundary layer
c	cooled wall conditions

0 free stream

1 inlet entrance conditions

2 conditions inside inlet and downstream of terminal shock

Barred values indicate a time-averaged quantity

APPENDIX B

DERIVATION OF INLET PERFORMANCE PARAMETERS FOR SCOOP OPERATING IN A TURBULENT BOUNDARY LAYER WITH WALL COOLING

Mass-Flow and Momentum Ratios

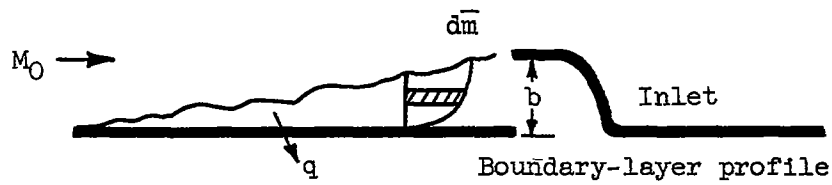

Sketch (a)

Mass-flow ratio derivation. - The incremental mass flow entering an inlet of height b (sketch (a)) and unity width submerged in a turbulent boundary layer with heat transfer is

$$d\bar{m} = \overline{\rho u}\, dy$$

and the mass flow entering the scoop is

$$\bar{m} = \delta \int_0^{b/\delta} \overline{\rho u}\, d\left(\frac{y}{\delta}\right) \tag{B1}$$

For an identical scoop operating in the free-stream, the captured mass flow would be

$$m_0 = \delta \int_0^{b/\delta} \rho_0 u_0\, d\left(\frac{y}{\delta}\right) \tag{B2}$$

and therefore, the ratio of equations (B1) and (B2) is

$$\frac{\bar{m}}{m_0} = \frac{\displaystyle\int_0^{b/\delta} \overline{\rho u}\, d\left(\frac{y}{\delta}\right)}{\displaystyle\int_0^{b/\delta} \rho_0 u_0\, d\left(\frac{y}{\delta}\right)} \tag{B3}$$

or when $b/\delta = 1.0$, and $\rho_0 u_0$ is constant,

$$\frac{\bar{m}}{m_0} = \int_0^1 \frac{\overline{\rho u}}{\rho_0 u_0} \, d\left(\frac{y}{\delta}\right) \tag{B4}$$

Momentum ratio derivation. - The momentum of the incremental mass (sketch 1)(for unity width) is

$$d\bar{\varphi} = \bar{u} \, d\bar{m} = \bar{\rho}(\bar{u})^2 \, dy$$

and the momentum of the mass entering the scoop is

$$\bar{\varphi} = \delta \int_0^{b/\delta} \bar{\rho}(\bar{u})^2 \, d\left(\frac{y}{\delta}\right) \tag{B5}$$

while the momentum of the mass captured in the free stream for an equivalent sized inlet would be

$$\varphi_0 = \delta \int_0^{b/\delta} \rho_0 u_0^2 \, d\left(\frac{y}{\delta}\right) \tag{B6}$$

and the boundary-layer momentum ratio when $b/\delta = 1$, and $\rho_0 u_0$ is constant becomes

$$\frac{\bar{\varphi}}{\varphi_0} = \int_0^1 \frac{\bar{\rho}}{\rho_0}\left(\frac{\bar{u}}{u_0}\right)^2 d\left(\frac{y}{\delta}\right) \tag{B7}$$

Mass and momentum ratios with wall cooling. - From the equation of state $p = \rho R t$ and the assumption that the static pressure remains constant through the boundary layer, the density ratio with heat transfer may be written as follows in terms of the velocity ratio $\bar{u}/u_0$ with the relationship from reference 2 (for a Prandtl number of unity)

$$\frac{\bar{\rho}}{\rho_0} = \frac{\bar{\rho}}{\rho_w}\frac{\rho_w}{\rho_0} = \frac{\bar{\rho}}{\rho_w}\frac{1}{\left(\frac{t_w}{t_0}\right)} = \frac{1}{\left(\frac{t_w}{t_0}\right)}\frac{1}{\left[1 + B\left(\frac{\bar{u}}{u_0}\right) - G^2\left(\frac{\bar{u}}{u_0}\right)^2\right]} \tag{B8}$$

where G and B are constants depending upon the free-stream Mach number M_0 and the wall-to-free-stream static temperature ratio (see appendix A).

The velocity distribution for a turbulent boundary layer with heat transfer, as developed in reference 2, is given as follows:

$$2.50\sqrt{\frac{M_0^2}{5}}\sqrt{C_{H,0}}\ln\left(\frac{y}{\delta}\right) = (\sin^{-1}v - \sin^{-1}v_0) \tag{B9}$$

where

$$\left.\begin{aligned} v &= \left[\frac{G}{a}\left(\frac{\bar{u}}{u_0}\right) - \frac{B}{2Ga}\right] \\ v_0 &= \left(\frac{G}{a} - \frac{B}{2Ga}\right) \end{aligned}\right\} \tag{B10}$$

In equation (B10), a, G, and B are defined according to appendix A.

By letting $N = 2.50\sqrt{\frac{M_0^2}{5}}\,C_{H,0}$ and by differentiating equation (B9),

$$d\left(\frac{y}{\delta}\right) = \exp\frac{1}{N}(\sin^{-1}v - \sin^{-1}v_0)\,\frac{dv}{\sqrt{1 - v^2}}\,\frac{1}{N} \tag{B11}$$

when $\alpha = \sin^{-1}v$ is used, (B11a)

$$d\alpha = \frac{dv}{\sqrt{1 - v^2}}, \quad \text{for} \quad -\frac{\pi}{2} < \alpha < \frac{\pi}{2}$$

and substitution in equation (B11) gives

$$d\left(\frac{y}{\delta}\right) = \exp\frac{1}{N}(\alpha - \alpha_0)\,\frac{d\alpha}{N} \tag{B12}$$

Since, from equation (B10),

$$\left(\frac{\bar{u}}{u_0}\right) = \left(\sin\alpha + \frac{B}{2Ga}\right)\frac{a}{G} \tag{B13}$$

equation (B8) becomes

$$\frac{\bar{\rho}}{\rho_0} = \frac{1}{\left(\frac{t_w}{t_0}\right)}\,\frac{1}{a^2\cos^2\alpha} \tag{B14}$$

By using equations (B11), (B12), and (B13) in equations (B4) and (B7), the expressions for boundary-layer mass flow and momentum ratio become

$$\frac{\bar{m}}{m_0} = Q\int_{\alpha_w}^{\alpha_0}\left(\sin\alpha + \frac{B}{2Ga}\right)\sec^2\alpha\,\exp\frac{\alpha}{N}\,d\alpha \tag{B15}$$

and

$$\frac{\bar{\varphi}}{\varphi_0} = \frac{aQ}{G}\int_{\alpha_w}^{\alpha_0}\left(\sin\alpha + \frac{B}{2Ga}\right)^2 \sec^2\alpha \exp\frac{\alpha}{N}\,d\alpha \qquad (B16)$$

where

$$Q = \frac{1}{GaN\left(\exp\frac{\alpha_0}{N}\right)}\frac{1}{\left(\frac{t_w}{t_0}\right)} \qquad (B16a)$$

and

$$\alpha_0 = \sin^{-1}v_0 = \sin^{-1}\left(\frac{G}{a} - \frac{B}{2Ga}\right)$$

Integration limits α_0 and α_w of equation (B15) and (B16) are found from the velocity conditions at the wall and at the outer edge of the boundary layer as follows: since

$$\alpha = \sin^{-1}v = \sin^{-1}\left[\frac{G}{a}\left(\frac{\bar{u}}{u_0}\right) - \frac{B}{2Ga}\right]$$

for $\frac{\bar{u}}{u_0} = 0$ at the wall

$$\alpha_w = \sin^{-1}\left(-\frac{B}{2Ga}\right)$$

and for $\frac{\bar{u}}{u_0} = 1$ at the outer edge of the boundary layer

$$\alpha_0 = \sin^{-1}\left(\frac{G}{a} - \frac{B}{2Ga}\right)$$

Estimation of Boundary-Layer Inlet Total-Temperature Ratio

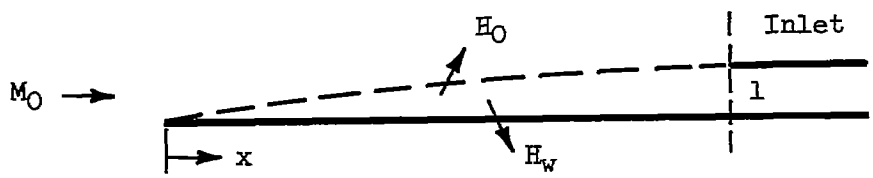

Sketch (b)

Flat-plate case. - Conservation of energy for the boundary-layer scoop model shown in sketch (b) may be written as

$$m_1 c_p T_0 - H_w - H_0 = m_1 c_p T_1 \qquad (B17)$$

where the second and third terms are the heat transfer rates out of the system. By definition and from reference 2 (for Prandtl number of 1) for unit width,

$$H_w = \int_0^x q_w \, dx = c_p \rho_0 u_0 (T_0 - t_w) \int_0^x C_{H,0} \, dx$$

where $C_{H,0}$ is the local heat-transfer coefficient on the plate. Since

$$2C_{H,0} = c_{f,0} = \frac{2\tau_w}{\rho_0 u_0^2}$$

then

$$\int_0^x \tau_w \, dx = \frac{C_{f,0} x}{2} = \int_0^x C_{H,0} \, dx$$

when $H_0 = 0$, equation (B17) becomes

$$\left(\frac{m_1}{m_0}\right) \rho_0 u_0 A_1 c_p T_0 - c_p \rho_0 u_0 (T_0 - t_w) \frac{C_{f,0} x}{2} = m_1 c_p T_1 \tag{B18}$$

Now for the flat plate

$$A_1 = (\delta) \times (\text{unity width})$$

and division of equation (B18) by $c_p T_0 \rho_0 u_0 \delta$ yields

$$\left(\frac{m_1}{m_0}\right) - \left(1 - \frac{t_w}{T_0}\right) \frac{C_{f,0} x}{2\delta} = \frac{m_1}{m_0} \frac{T_1}{T_0} \tag{B19}$$

Note that $m_1 = \bar{m}$ and $\bar{\varphi} = \varphi_1$ at the inlet. Now rearrangement of equation (B19) will make

$$\frac{C_{f,0} x}{2\delta} = \left(\frac{\bar{m}}{m_0} - \frac{\bar{\varphi}}{\varphi_0}\right)$$

From equation (C2) of appendix C, the inlet total-temperature ratio becomes

$$\frac{T_1}{T_0} = 1 - \left(1 - \frac{t_w}{T_0}\right)\left[1 - \frac{\left(\frac{\bar{\varphi}}{\varphi_0}\right)}{\left(\frac{\bar{m}}{m_0}\right)}\right] \tag{B20}$$

Conical case. - In appendix C, the following relation between the mean skin-friction coefficient and the inlet parameters of figure 1 was found from equation (C4)

$$\frac{C_{f,0}x}{4\delta} = \left(\frac{\bar{m}}{m_0} - \frac{\bar{\varphi}}{\varphi_0}\right)$$

Now, if the inlet capture area of a scoop (on a cone) is approximated by $A_1 \approx 2\pi x \sin\theta\ \delta$, substitution of these relations in equation (B17) yields an expression identical to that of the flat plate (eq. (B20)). Variation of this temperature ratio with Mach number for various Reynolds numbers and for a wall-to-free-stream static-temperature ratio of unity is presented in figure 2.

Boundary-Layer Inlet Total-Pressure Recovery Estimation

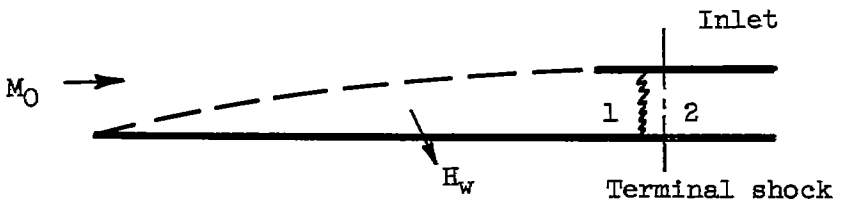

Sketch (c)

A one-dimensional representation of uniform flow inside an inlet and behind a normal shock can now be made from the mass flow and total momentum for the system of sketch (c). From conservation of mass and momentum these equations are,

$$\left(\frac{\bar{m}}{m_0}\right)\frac{p_0 A_2 M_0 \sqrt{1 + \frac{\gamma - 1}{2} M_0^2}}{\sqrt{T_0}} = \frac{p_2 A_2 M_2 \sqrt{1 + \frac{\gamma - 1}{2} M_2^2}}{\sqrt{T_2}}$$

and

$$p_0\left(\frac{\Phi}{\Phi_0}\right) A_2(1 + \gamma M_0^2) = p_2 A_2(1 + \gamma M_2^2)$$

respectively. The subscript 2 now denotes a condition behind the normal shock. A division of the second equation by the first gives the following:

$$\frac{\left(\frac{\Phi}{\Phi_0}\right)}{\left(\frac{\bar{m}}{m_0}\right)} \frac{(1 + \gamma M_0^2)\sqrt{T_0}}{M_0 \sqrt{1 + \frac{\gamma - 1}{2} M_0^2}} = \frac{(1 + \gamma M_2^2)\sqrt{T_2}}{M_2 \sqrt{1 + \frac{\gamma - 1}{2} M_2^2}} \qquad \text{(B21)}$$

and a division of both sides by $\sqrt{2(\gamma + 1}$ gives an expression similar to that in reference 1 (appendix C) obtained (for $T_1 = T_2$), namely;

$$\frac{\left(\frac{\Phi}{\Phi_0}\right)\left(\frac{F}{F_*}\right)_0}{\left(\frac{\bar{m}}{m_0}\right)\sqrt{\frac{T_1}{T_0}}} = \left(\frac{F}{F_*}\right)_2 \tag{B22}$$

where

$$\left(\frac{F}{F_*}\right) = \frac{1 + \gamma M^2}{M\sqrt{1 + \frac{\gamma - 1}{2} M^2}} \frac{1}{\sqrt{2(\gamma + 1)}}$$

and

$$\frac{\Phi}{\Phi_0} = \frac{1 + \gamma \frac{\bar{\Phi}}{\Phi_0} M_0^2}{(1 + \gamma M_0^2)}$$

Since all the conditions on the left hand side of equation (B22) are known or can be found, the inlet Mach number M_2 behind the terminal shock and corresponding to a normal shock-type inlet may be found. The total-pressure recovery ratio P_2/P_0 is found from the mass-flow equation as

$$\frac{P_2}{P_0} = \left(\frac{\bar{m}}{m_0}\right) \frac{\left(\frac{A_*}{A}\right)_0}{\left(\frac{A_*}{A}\right)_2} \sqrt{\frac{T_1}{T_0}} \tag{B23}$$

Variation of this pressure ratio, which includes the effect of mixing losses, is plotted in figure 3 for various Reynolds and Mach numbers and for the adiabatic and wall-to-local stream temperature ratio of unity.

APPENDIX C

CALCULATION OF ADIABATIC-TO-COOLED BOUNDARY-LAYER THICKNESS RATIO

Flat-Plate Case

As presented in reference 2,

$$\delta = \frac{C_{f,0}x}{2} \frac{1}{\int_0^1 \frac{\bar{\rho}}{\rho_0} \frac{\bar{u}}{u_0} \left(1 - \frac{\bar{u}}{u_0}\right) d\left(\frac{y}{\delta}\right)} \tag{C1}$$

where $C_{f,0}$ = mean skin-friction coefficient and x = distance along surface. Since

$$\frac{\bar{m}}{m_0} = \int_0^1 \frac{\overline{\rho u}}{\rho_0 u_0} d\left(\frac{y}{\delta}\right)$$

and

$$\frac{\bar{\varphi}}{\varphi_0} = \int_0^1 \frac{\bar{\rho}}{\rho_0}\left(\frac{\bar{u}}{u_0}\right)^2 d\left(\frac{y}{\delta}\right)$$

from equations (B4) and (B7). Then in equation (C1),

$$\delta = \frac{C_{f,0}x}{2} \frac{1}{\left(\frac{\bar{m}}{m_0} - \frac{\bar{\varphi}}{\varphi_0}\right)} \tag{C2}$$

and the adiabatic-to-cooled boundary-layer thickness ratio is

$$\frac{\delta_{ad}}{\delta_c} = \frac{C_{f,0_{ad}}}{C_{f,0_c}} \frac{\left(\frac{\bar{m}}{m_0} - \frac{\bar{\varphi}}{\varphi_0}\right)_c}{\left(\frac{\bar{m}}{m_0} - \frac{\bar{\varphi}}{\varphi_0}\right)_{ad}} \tag{C3}$$

Cone Case

Since from reference 3,

$$\tau_w = \rho_0 u_0^2 \left[\frac{d}{dx} \int_0^\delta \frac{\overline{\rho u}}{\rho_0 u_0} \left(1 - \frac{\bar{u}}{u_0}\right) dy + \frac{1}{x} \int_0^\delta \frac{\overline{\rho u}}{\rho_0 u_0} \left(1 - \frac{\bar{u}}{u_0}\right) dy \right]$$

then

$$\int_0^x \tau_w x \, dx = \delta \rho_0 u_0^2 x \int_0^1 \frac{\overline{\rho u}}{\rho_0 u_0} \left(1 - \frac{\bar{u}}{u_0}\right) d\left(\frac{y}{\delta}\right)$$

4607

Now

$$\int_0^x \tau_w x \, dx = \frac{1}{2} C_{f_w} \rho_w u_0^2 \left(\frac{x^2}{2}\right)$$

or

$$\frac{1}{2} C_{f_w} (\rho_w u_0^2) \frac{x^2}{2} = \delta x \int_0^1 \frac{\overline{\rho u}}{\rho_0 u_0} \left(1 - \frac{\bar{u}}{u_0}\right) d\left(\frac{y}{\delta}\right) (\rho_0 u_0^2)$$

so that

$$\delta = \frac{1}{4} \frac{C_{f,0} x}{\int_0^1 \frac{\overline{\rho u}}{\rho_0 u_0} \left(1 - \frac{\bar{u}}{u_0}\right) d\left(\frac{y}{\delta}\right)} \qquad (C4)$$

Therefore, the adiabatic-to-cooled boundary-layer thickness ratio would be the same as that for the flat plate (eq. (C3)) except that the mean skin-friction coefficient is evaluated for a cone.

REFERENCES

1. Simon, Paul C., and Kowalski, Kenneth L.: Charts of Boundary-Layer Mass Flow and Momentum for Inlet Performance Analysis - Mach Number Range 0.2 to 5.0. NACA TN 3583, 1955.

2. Van Driest, E. R.: Turbulent Boundary Layer in Compressible Fluids. Jour. Aero. Sci., vol. 18, no. 3, Mar. 1951, pp. 145-161.

3. Van Driest, E. R.: Turbulent Boundary Layer on a Cone in a Supersonic Flow at Zero Angle of Attack. Jour. Aero. Sci., vol. 19, no. 1, Jan. 1952, pp. 55-57; 72.

TABLE I. - EFFECT OF γ ON INLET FLOW PARAMETERS

Re_0	M_0	γ_{bl}	t_w/t_0	$\bar{m}/m_0$	$\bar{\varphi}/\varphi_0$	P_2/P_0[b]
10^6	10	1.1	[a]6.0	0.540	0.505	14.8×10^{-4}
		1.2	[a]11.0	.421	.397	11.8
		1.3	[a]16.0	.345	.327	9.75
		1.4	[a]21.0	.304	.290	8.7
		1.4	1.0	.48	.44	13.4

[a]Adiabatic wall conditions

[b]$\gamma = 1.4$; $\gamma_2 = 1.1$

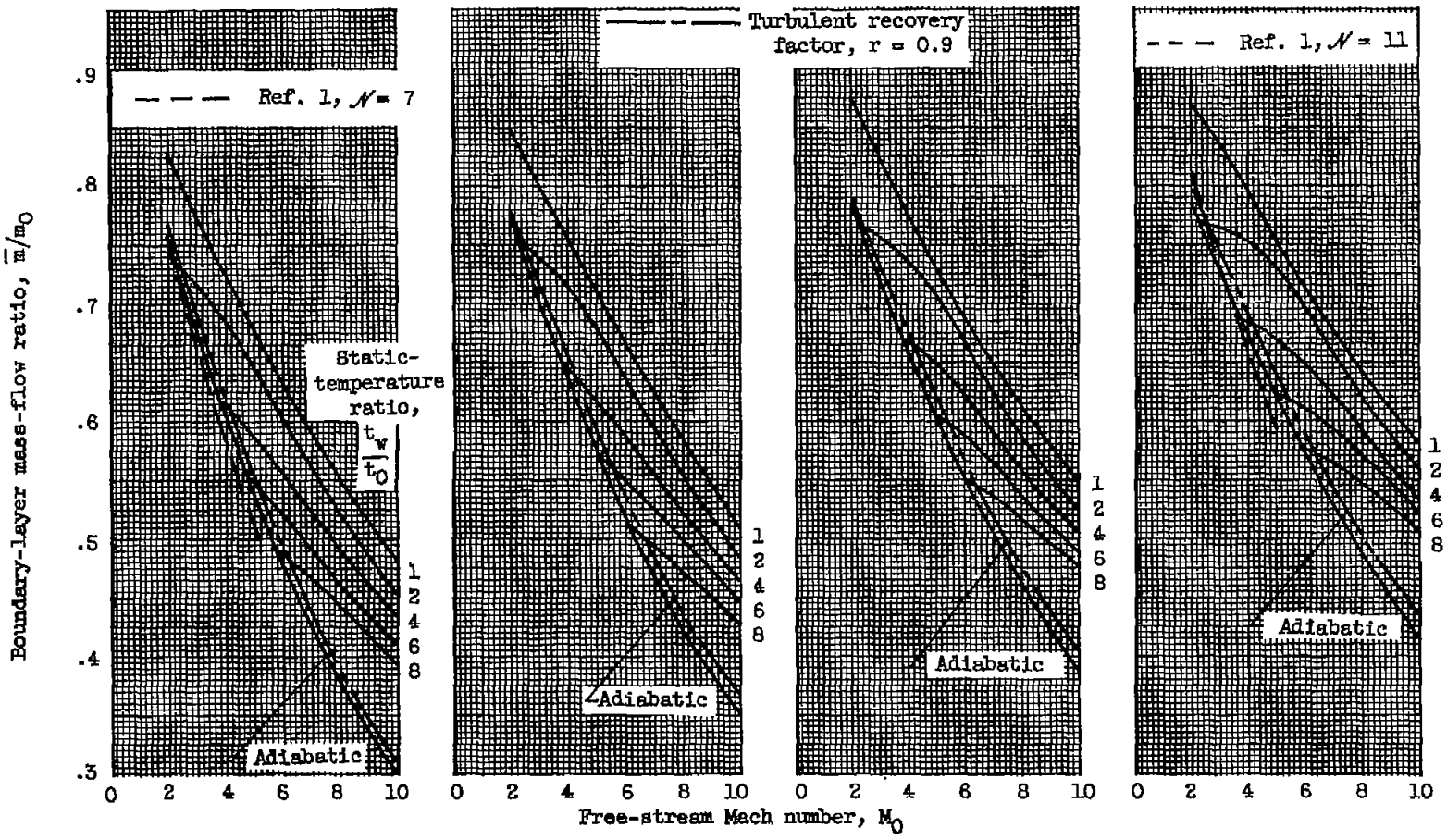

(a) Mass-flow ratio.

Figure 1. - Variation of boundary-layer mass-flow and momentum ratios with local Mach number for various Reynolds numbers and temperature ratios on flat and conical surfaces.

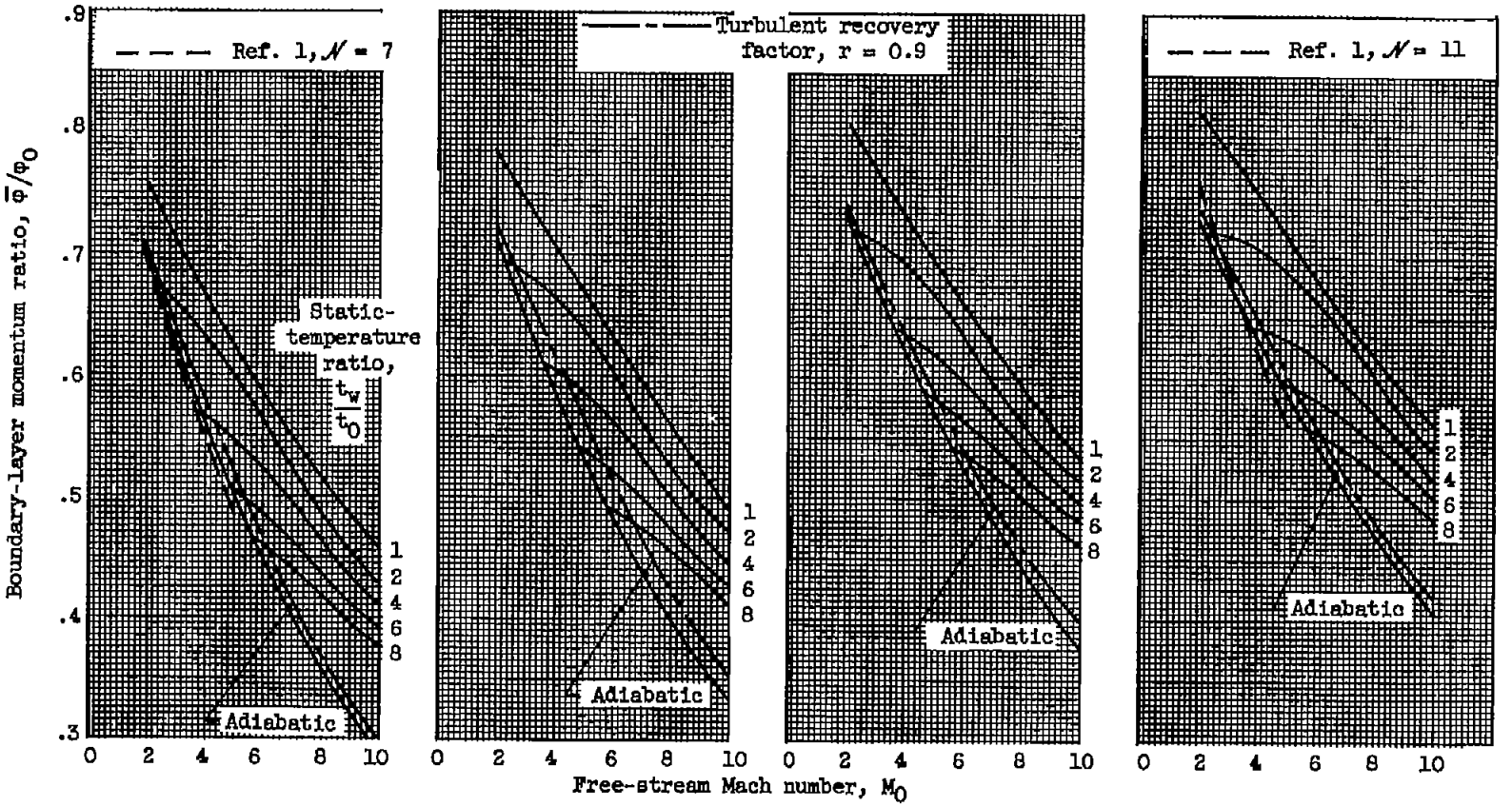

(a) $Re_0 = 10^6$. (b) $Re_0 = 10^7$. (c) $Re_0 = 10^8$. (d) $Re_0 = 10^9$.

(b) Momentum ratio.

Figure 1. - Concluded. Variation of boundary-layer mass-flow and momentum ratios with local Mach number for various Reynolds numbers and temperature ratios on flat and conical surfaces.

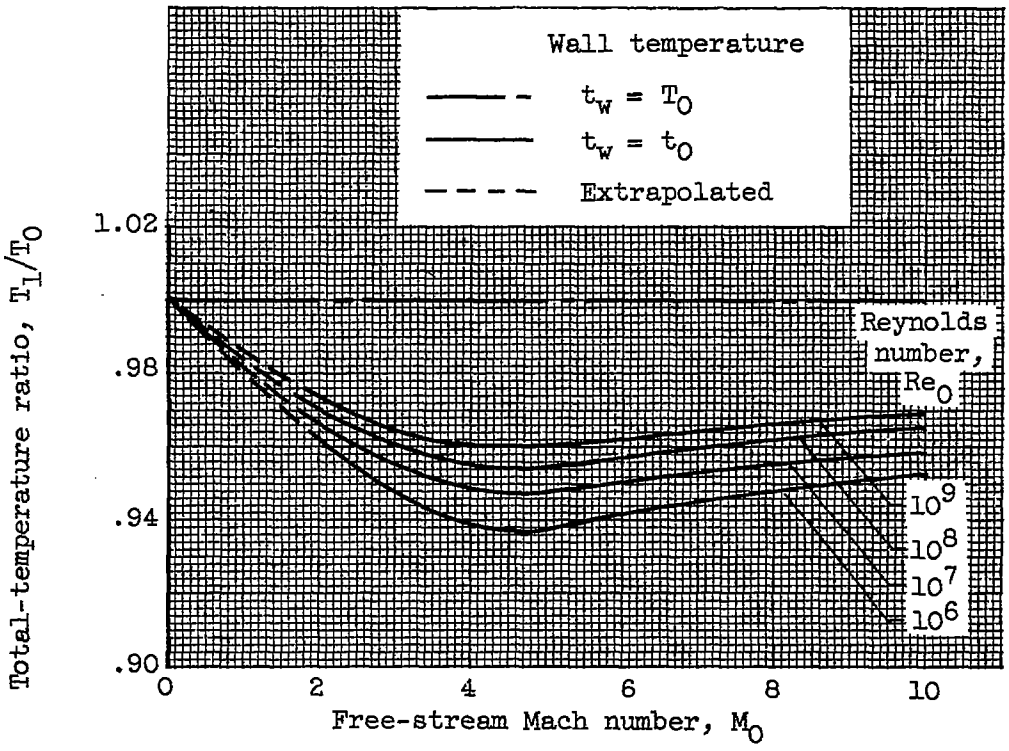

Figure 2. - Variation of boundary-layer inlet total-temperature ratio with local Mach number; Prandtl number, 1.0.

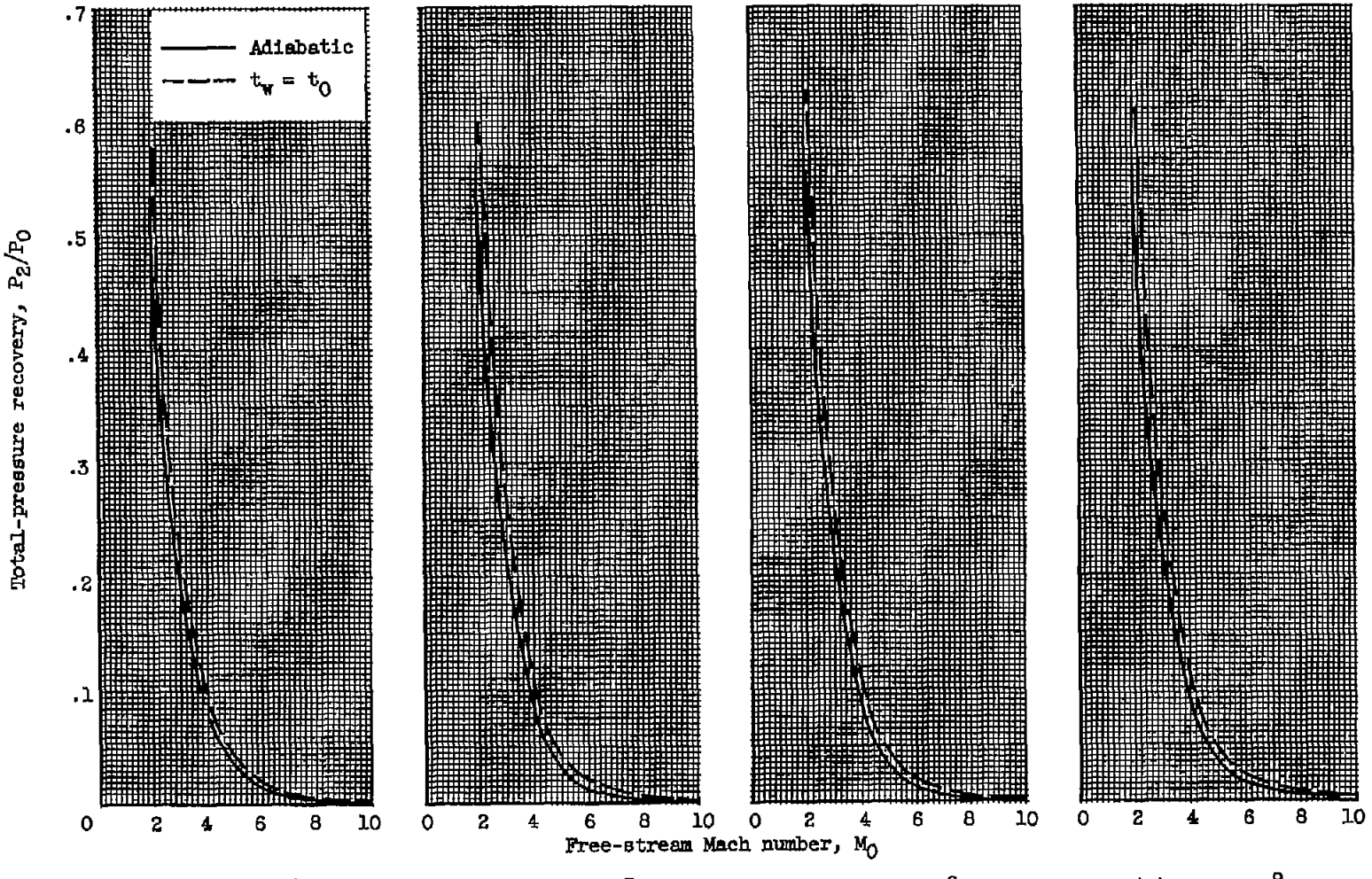

(a) $Re_0 = 10^6$. (b) $Re_0 = 10^7$. (c) $Re_0 = 10^8$. (d) $Re_0 = 10^9$.

Figure 3. - Critical total-pressure recovery of normal shock-type scoop inlet.